Pharmacology & Pharmacy, 2023, 14, 156-175
https://www.scirp.org/journal/pp
ISSN Online: 2157-9431
ISSN Print: 2157-9423

Role of Polyethylene Glycol and Silica for Dissolution Enhancement of Cefuroxime Axetil: *In-Vitro* Performance Evaluation and Characterization

Mst. Boby Aktar Bithy[1], Milon Kumar Ghosh[2], Ashim Kumar[1], Md. Rafiqul Islam Khan[1], Mir Imam Ibne Wahed[1], Ranjan Kumar Barman[1*]

[1]Laboratory of Pharmaceutics, Department of Pharmacy, Faculty of Science, University of Rajshahi, Rajshahi, Bangladesh
[2]Department of Pharmacy, Faculty of Biological Sciences, Islamic University, Kushtia, Bangladesh
Email: *drbarman76@gmail.com

How to cite this paper: Bithy, Mst.B.A., Ghosh, M.K., Kumar, A., Khan, Md.R.I., Wahed, M.I.I. and Barman, R.K. (2023) Role of Polyethylene Glycol and Silica for Dissolution Enhancement of Cefuroxime Axetil: *In-Vitro* Performance Evaluation and Characterization. *Pharmacology & Pharmacy*, **14**, 156-175.
https://doi.org/10.4236/pp.2023.145012

Received: March 30, 2023
Accepted: May 20, 2023
Published: May 23, 2023

Abstract

Cefuroxime Axetil (CA) a widely used cephalosporin antibiotic displays low aqueous solubility and high membrane penetrability. This results in its solubility driven variable and/or low oral bioavailability and therapeutic efficacy as a major drawback. Thus, most of the goal of our study was to increase the solubility as well as dissolution rate of CA using the simple and cost-effective solid dispersion (SD) method. At first, the SD formulations of CA were prepared at various weight ratios of Carplex-67 and PEG-4000 by solvent evaporation technique. These new formulations were then subjected to an *in-vitro* drug release performance study and tested for physicochemical characterization to distinguish the thermal behavior, crystallinity, interactions phenomena, and surface morphology. Among the formulated Cefuroxime Axetil Solid Dispersion (CSD), CSD-8 which contained CA, Carplex-67, and PEG-4000 at the weight ratio 1:3:2, respectively showed the most significant ($p < 0.001$) drug release that was about 2.11 times higher, although all CSD was better than pure CA. The physicochemical studies revealed that no unusual interactions were found in the CSD formulations and the increased dissolution resulted from the amorphous conversion of CA and better wettability upon CSD formulation. Finally, the optimized formulation (CSD-8) was compared with the marketed preparation in terms of *in-vitro* dissolution in water, Gastric Simulated Fluid (GSF), and Intestinal Simulated Fluid (ISF). This study also showed a significant ($p < 0.001$) increase in drug release compared to the marketed product. Therefore, it is supposed to be a promising alternative to conventional antimicrobial therapy.

Keywords

Carplex-67, Cefuroxime Axetil, Improved Dissolution, PEG-4000, Solid Dispersion, Solvent Evaporation

1. Introduction

Cefuroxime Axetil (CA) is the first commercially available cephalosporin antibiotic derived from cephalosporin's 7-cephalosporanic acid nucleus, which is an acetoxyethyl ester prodrug of Cefuroxime that is active against both gram-positive and gram-negative bacteria [1]. The chemical name of CA is 1-acetoxyethyl (6R, 7R)-3-(carbamoyloxymethyl)-7-[[(2E)-2-(furan-2-yl)-2-methoxyiminoacetyl]ami -no]-8-oxo-5-thia-1-azabicyclo [4.2.0] oct-2-ene-2 carboxylate [2]. It is widely used to treat gonorrhea, acute bacterial otitis, pharyngitis, tonsillitis, acute maxillary sinusitis, meningitis, ear infections, bone, and joint infections, and mild to moderate respiratory tract infections. The treatment of individuals with genitourinary, skin, and soft tissue infections, as well as erythema migraines linked to an early stage of Lyme disease, is also successful with CA. Additionally, it is less dangerous than penicillin and other cephalosporin antibiotics because it does not increase allergic reactions [3]. After oral administration, the prodrug CA is promptly hydrolysed by esterase in the intestinal mucosa to produce active Cefuroxime. Because of its limited water solubility (as it is a BCS class II drug), it shows dissolving difficulties in the stomach and intestinal fluids, resulting in limited dissolution, hence poor bioavailability. As a result, physical modification is required to increase CA's water solubility to maximize its therapeutic effects [4]. Particle size reduction by micronization and nano-suspension; crystal habit modification, e.g., polymorphs; pseudopolymorph; nanocrystal; amorphous form; complexation or solubilization using cyclodextrin and surfactants, as well as drug dispersion in carriers like eutectic mixtures; solid dispersion and solid solutions are all common physical phenomena for increasing solubility [5]. In this case, solid dispersion technology is being utilized to improve the solubility of poorly water-soluble pharmaceuticals [6]. Solid dispersions (SDs) are a form of solid product that comprises at least two different components, usually a hydrophilic matrix and a hydrophobic medicament, and are originally developed in the early 1990s. The drug can be molecularly distributed in both amorphous (clusters) and crystalline particles, and the matrix can be crystalline or amorphous [7]. Due to an increase in the number of FDA-approved medicines in recent years, SDs are now widely recognized as a platform technology for the formulation of poorly soluble medications [8]. The drug release profile in SDs can be improved by manipulating the carrier and SDs particle properties [9]. By modifying particle size distribution and enhancing wettability, porosity, and polymorphism change, SDs also improve medication bioavailability [10]. This approach has also proven to be effective in the development of formulations with a

high loading capacity for medicines with a tendency to recrystallize [8]. For the preparation of SDs, many procedures have been documented, including fusion, solvent evaporation, solvent wetting, spray drying, and hot-melt extrusion [11] [12]. Because of its simplicity, the solvent evaporation method is the most convenient for making SDs. To get the expected SDs, this procedure involves dissolving the medication and carrier in a suitable solvent, then evaporating the solvent [10]. A number of hydrophilic carriers have been used to increase the dissolving properties and bioavailability of medicines that are poorly water-soluble [13] [14]. The main aspiration of this study was to improve the solubility and rate of dissolution of CA by using Carplex-67 and PEG 4000 as carriers. No prior evidence of employing such carriers with CA was found. Cefuroxime Axetil: Carplex-67: PEG-4000 formulations produced by the solvent evaporation method enhance medication dissolving rates from solid dispersions as compared to the pure drug.

2. Materials and Methods

2.1. Materials

Square Pharmaceuticals Ltd., Pabna, Bangladesh, delivered CA (Atom pharma, Gujarat, India) as a gracious gift. Silica (Carplex 67) and Polyethylene glycol (PEG-4000) were purchased from Evonik Pvt. Ltd. (Hanua, Germany) and Qualikems Fine Chem Pvt. Ltd. (India) respectively. Cefuroxime Axetil 500 mg tablets were procured from Rajshahi City from four separate pharmacies. The remainder of the chemicals and solvents were of analytical grade.

2.2. Preparation of Solid Dispersions of CA

The solvent evaporation method was used to make solid dispersion formulations of CA (CSDs) utilizing Carplex-67 and polyethylene glycol-4000 alone and in combination. In a beaker, correctly weighed (100 mg) CA was dissolved in a suitable amount of acetone before the individual dispersion carrier was added at varying ratios (**Table 1**). The dispersion solution was then stirred continuously at 250 rpm with a magnetic stirrer (Wisd, Korea) to allow sufficient drug loading into carriers. To evaporate the solvent from the dispersion system, the temperature was kept at 50˚C - 60˚C. The magnetic stirrer was turned off when the solvent evaporation was nearly complete, and the CSDs were obtained as a dried powder at room temperature. All of the CSDs were stored in an airtight container.

2.3. Determination of the Percentage of Yield

Using the following equation, the percentage of yield was estimated from the weight of dried CSDs (W_2 = Obtained weight) recovered from each batch and the sum of the original dry weight of starting materials (W_1 = Theoretical weight).

$$\text{Yield}(\%) = \frac{W_2}{W_1} \times 100 \quad (1)$$

Table 1. Drug–carrier ratio of the prepared solid dispersion.

Formulation	Drug & Carrier	Ratio
CSD-1	CA: Carplex-67	1:1
CSD-2	CA: Carplex-67	1:2
CSD-3	CA: Carplex-67	1:2.5
CSD-4	CA: Carplex-67	1:3
CSD-5	CA: Carplex-67	1:4
CSD-6	CA: Carplex-67: PEG-4000	1:3:0.5
CSD-7	CA: Carplex-67: PEG-4000	1:3:1
CSD-8	CA: Carplex-67: PEG-4000	1:3:2

2.4. Estimation of Encapsulation Efficiency

The improvised methodology described by Mouffok M *et al.* [15] was used to measure the encapsulation efficiency (EE) of CSDs. A total of 100 mg of CSDs were precisely weighed and dissolved in 100 mL methanol. The solution was forcefully agitated and filtered, with the filtrate being spectrophotometrically (UVmini-1240, Shimadzu, Japan) evaluated for CA concentration at 281 nm. Using the formula below, the amount of CA encapsulated in the CSDs was determined to achieve the percent encapsulation efficiency:

$$\mathrm{EE}(\%) = \frac{\text{Actual Drug Content}}{\text{Theoretical drug content}} \times 100 \quad (2)$$

The above procedure was repeated in triplicate to obtain the encapsulation efficiency from the mean.

2.5. Dissolution Study

The *in-vitro* dissolution investigation was carried out utilizing a dissolution tester (Tianjin Guoming Medicinal Equipment Co., Ltd.) and de-mineralized (DM) water as the dissolution medium for both pure CA and CSDs [16] [17]. In a nutshell, a sample of CSDs containing 13.5 mg of CA was placed in Fisherbrand dialysis tubing (Fisherbrand™ Regenerated Cellulose Dialysis Tubing, MW: 12,000 - 14,000; width: 45 mm; wall thickness: 20 μm; dry cylinder diameter: 28.6 mm; volume/cm: 6.42) and immersed in 900 ml of dissolution medium enclosed in a dissolution tube at 37.0˚C ± 0.5˚C and 100 ± 2 rpm. Periodically, analyte samples were taken and replaced with an equivalent volume of fresh dissolving media. Using a calibration curve (**Figure 1**), the concentration of CA at each point (5 μg/ml, 10 μg/ml, 20 μg/ml, 30 μg/ml, and 50 μg/ml) was determined by measuring absorbance at 281 nm with a UV-spectrophotometer.

2.6. Solid-State Characterization of CSDs

2.6.1. Differential Scanning Calorimetry (DSC)

DSC (Seiko Instruments inc. Tokyo, Japan) was used to acquire thermo-grams of CA, different additives, and CSDs. Each sample (10 mg) was placed in sealed

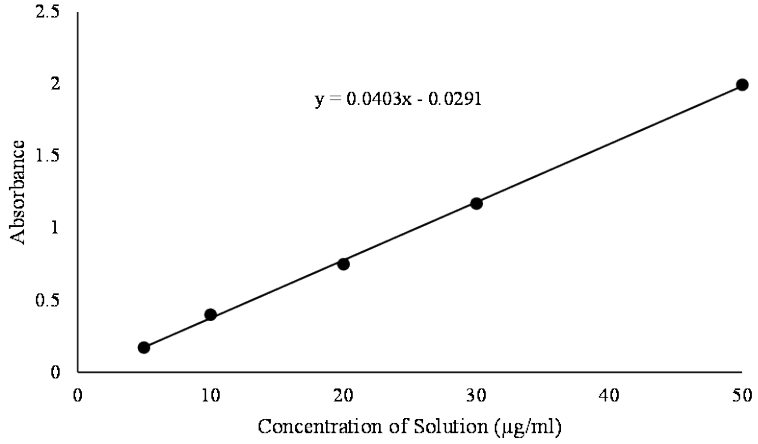

Figure 1. Calibration curve of Cefuroxime Axetil.

standard aluminium pans and heated from 30˚C - 300˚C at a scanning rate of 10˚C/min under nitrogen purge with an empty aluminium pan as a reference [18].

2.6.2. Powder X-Ray Diffractometer (PXRD)

The diffraction investigation was conducted using an X-ray diffractometer (Rigaku Corporation Mini Flex II Tokyo, Japan). The CSDs and CA were subjected to Cu-K radiation (30 kV and 50 mA) and scanned from 2 to 40, and 2θ degrees at a rate of 5 degrees per minute [18].

2.6.3. Fourier Transform Infrared Spectroscopy (FTIR)

IR spectra recorded using the diffuse reflection method using an FTIR spectrometer (Shimadzu Corporation IR Prestige-21, Techno Science dura Samp1IR Japan) were used to explore the nature of drug-carrier interactions in CSDs. Grounding and thorough mixing with potassium bromide was used to prepare the disks of samples. The resolution was 4.0 cm^{-1} with a scanning range of 500 to 4000 cm^{-1} [18].

2.6.4. Scanning Electron Microscopy (SEM)

After platinum metallization, the shape, surface, and cross-sectional morphology of CA and CSDs were examined using a scanning electron microscope (Hitachi High-tech Corporation TM3030, Japan). A 15 kV accelerating voltage was used [18].

2.6.5. Comparing Drug Release from Developed CSD with Marketed Products CAMPs (CA Marketed Products)

The marketed drugs were lightly triturated with a dried mortar and pestle, placed into a dialysis bag, and dissolving studies were conducted independently using DM (Demineralized) water, 0.1N HCl (GSF), and phosphate buffer pH 6.8 (ISF).

2.7. Statistical Analysis

The mean and standard error of the mean (SEM) were used to express the find-

ings. Graph Pad Prism 8.0.1 (Graphpad Software, Boston, USA) was used to examine differences across groups using an unpaired t-test. Statistical significance was defined as a value of $p < 0.05$.

3. Results

3.1. Percentage of Yield by CSDs

The percent yields derived from CSDs are shown in **Table 2** and in **Figure 2(a)**. The percent yields were ranging from 86.35% w/w (CSD-1) to 92.98% w/w (CSD-8). The highest yield obtained from CSD-8 indicated that the manufacturing technique adopted might be reliable and amendable to validation consistency [19] [20].

3.2. Encapsulation Efficiency

One of the most crucial factors in the formulation of drug nanoparticles is encapsulation efficiency because it directly reflects the concentration of active substances (drugs, proteins, antimicrobial agents, etc.) [21] [22]. **Table 2** and **Figure 2(b)** summarize the encapsulation efficiency of all CSDs. Among CSDs, CSD-8 containing Carplex-67 and PEG-4000 had a good encapsulation efficiency. This could be owing to carriers' high adsorption efficiency to the medication.

Table 2. Percentage of yields, and encapsulation efficiency of CSDs.

Formulations	Yield (%)	Encapsulation Efficiency (%)
CSD-1	86.35 ± 0.03	79.30 ± 0.96
CSD-2	87.16 ± 0.02	84.83 ± 0.93
CSD-3	88.63 ± 0.01	85.67 ± 0.73
CSD-4	90.70 ± 0.01	91.20 ± 0.44
CSD-5	87.52 ± 0.01	86.67 ± 0.88
CSD-6	89.11 ± 0.04	90.00 ± 0.58
CSD-7	89.84 ± 0.03	91.00 ± 1.53
CSD-8	92.98 ± 0.01	94.43 ± 0.57

Results are presented as mean ± S.E.M.

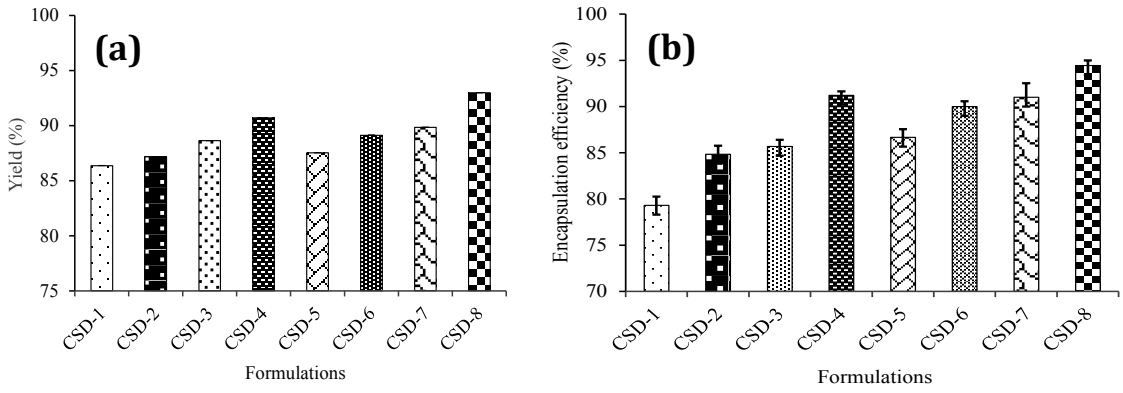

Figure 2. (a) Percentage of yields of CSDs. (b) Encapsulation efficiency of CSDs.

3.3. Dissolution Study

The release pattern of CA from CSDs was demonstrated using a dissolution study. To examine the drug release pattern, the formed CSDs were subjected to a dissolving analysis, and the dissolution profiles were created alongside those of pure CA. The best CSDs were identified based on the release pattern (*in-vitro* dissolution).

3.3.1. Dissolution Profiles of CSDs Containing Carplex-67

Table 3 and Figure 3 show the dissolution profiles of various CSDs. At the initial sample point (0 minute), all CSD formulations were releasing more drugs than pure CA and increased release by 1.04, 1.34, 1.15, 1.75, and 1.25 times more than pure CA. Pure CA concentration was 1.37 g/ml after 1 hour, while CSD-1, CSD-2, CSD-3, CSD-4, and CSD-5 concentrations were 1.43, 1.41, 1.64, 1.73, and 1.42 g/ml, respectively. In addition, CSD-1, CSD-2, CSD-3, CSD-4, and CSD-5 yielded peak concentrations of 9.94, 8.91, 9.34, 10.21, and 8.96 g/ml at 600 minutes, respectively.

Table 3. Dissolution profiles of CSDs containing carplex-67.

Time (min)	Concentration (µg/ml)					
	CA	CSD-1	CSD-2	CSD-3	CSD-4	CSD-5
0	0.25 ± 0.01	0.26 ± 0.01*	0.34 ± 0.02**	0.28 ± 0.017*	0.44 ± 0.017**	0.30 ± 0.02**
5	0.35 ± 0.01	0.37 ± 0.01	0.45 ± 0.02	0.36 ± 0.01	0.50 ± 0.025	0.41 ± 0.02
30	0.92 ± 0.02	0.94 ± 0.01	0.97 ± 0.01	0.97 ± 0.017	1.06 ± 0.017	0.98 ± 0.01
90	1.95 ± 0.01	1.98 ± 0.01	2.21 ± 0.05	1.97 ± 0.01	2.59 ± 0.017	2.22 ± 0.06
150	2.84 ± 0.02	3.07 ± 0.01	3.29 ± 0.02	3.57 ± 0.017	4.02 ± 0.025	3.41 ± 0.06
210	3.48 ± 0.01	3.74 ± 0.01	3.89 ± 0.02	4.78 ± 0.042	5.04 ± 0.035	4.51 ± 0.01
270	4.35 ± 0.02	4.76 ± 0.02*	4.89 ± 0.01*	5.29 ± 0.025**	6.16 ± 0.019***	5.93 ± 0.03**
330	4.74 ± 0.01	6.18 ± 0.01	5.83 ± 0.03	6.48 ± 0.025	7.25 ± 0.025	6.57 ± 0.04
420	5.20 ± 0.01	7.67 ± 0.01	7.23 ± 0.010	7.86 ± 0.03	8.86 ± 0.017	7.63 ± 0.01
510	5.63 ± 0.02	9.17 ± 0.03	8.29 ± 0.019	8.88 ± 0.017	9.72 ± 0.01	8.25 ± 0.00
600	6.10 ± 0.01	9.94 ± 0.01**	8.91 ± 0.017*	9.34 ± 0.023**	10.21 ± 0.01***	8.96 ± 0.01*

Results are presented as mean ± S.E.M. *p < 0.05, **p < 0.01, ***p < 0.001 vs. CA.

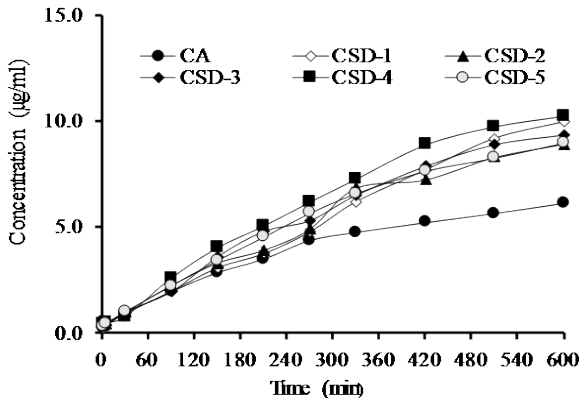

Figure 3. Dissolution profile of CA, CSD-1, CSD-2, CSD-3, CSD-4, and CSD-5. Each value represents mean ± S.E.M (n = 3).

Among these CSDs, CSD-4 produced significantly ($p < 0.001$) higher drug concentration in comparison to that of CSD-1, CSD-2, CSD-3, and CSD-5. Inferring the best formulation consisting of CA and silica (Caplex-67) at a ratio of 1:3 for maximizing CA dissolution based on the amount of relevance for drug release among different CSDs.

3.3.2. Dissolution Profiles of CSDs Containing Carplex-67 and PEG-4000

The CSD-4 was chosen for further research using both Carplex-67 and PEG-4000 at different ratios to produce CSD-6, CSD-7, and CSD-8 from the silica (Carplex-67) based CSDs. Table 4 and Figure 4 show the dissolution profiles of certain CSDs. The CSDs released 1.25, 1.26, and 2.11 times more drugs than pure CA significantly. CA, on the other hand, reached a peak concentration of 6.10 g/ml after 600 minutes. CSD-6 exhibited a comparable peak drug concentration to CA at 390 minutes, CSD-7 at 330 minutes, and CSD-8 at 210 minutes, suggesting that CSD-6, CSD-7, and CSD-8 were capable of quicker drug release in water. Despite this, the peak concentration produced by CSD-6, CSD-7, and CSD-8 was 9.34, 9.53, and 12.26 μg/ml at 600 minutes, respectively.

Table 4. Dissolution profile of CSDs containing carplex-67 and PEG-4000.

Time (min)	Concentration (μg/ml)			
	CA	CSD-6	CSD-7	CSD-8
0	0.25 ± 0.01	0.30 ± 0.02*	0.31 ± 0.03**	0.53 ± 0.02***
5	0.35 ± 0.01	0.39 ± 0.01	0.39 ± 0.01	0.63 ± 0.02
30	0.92 ± 0.01	0.97 ± 0.01	1.04 ± 0.01	1.15 ± 0.02
90	1.95 ± 0.01	1.97 ± 0.02	2.14 ± 0.05	3.28 ± 0.03
150	2.84 ± 0.01	2.93 ± 0.02	3.24 ± 0.03	4.93 ± 0.03
210	3.48 ± 0.01	3.51 ± 0.01	4.19 ± 0.02	6.34 ± 0.02
270	4.35 ± 0.02	4.42 ± 0.03*	5.07 ± 0.02**	7.85 ± 0.02***
330	4.74 ± 0.01	5.44 ± 0.03	6.03 ± 0.02	8.97 ± 0.02
420	5.20 ± 0.01	6.77 ± 0.01	7.15 ± 0.04	10.89 ± 0.01
510	5.63 ± 0.03	7.97 ± 0.01	8.48 ± 0.02	11.74 ± 0.02
600	6.10 ± 0.01	9.34 ± 0.02*	9.53 ± 0.02**	12.26 ± 0.02***

Results are presented as mean ± S.E.M. *$p < 0.05$, **$p < 0.01$, ***$p < 0.001$ vs. CA.

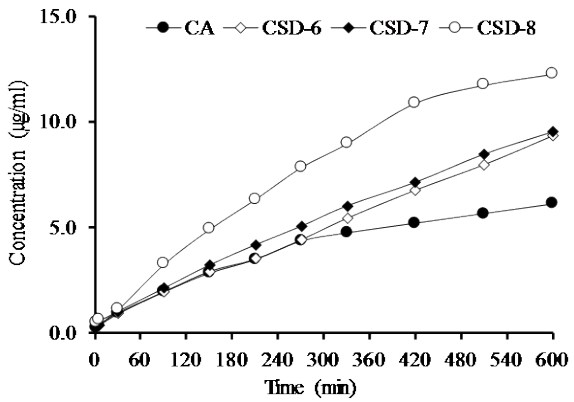

Figure 4. Dissolution profile of CA, CSD-6, CSD-7, and CSD-8. Each value represents mean ± S.E.M (n = 3).

CSD-8 produced significantly ($p < 0.001$) higher drug concentrations than CSD-6 and CSD-7. Considering the amount of relevance for drug release among different CSDs, CSD-8 could be inferred as the optimal formulation for optimizing CA dissolution, consisting of CA, silica, and PEG-4000 at a ratio of 1:3:2.

3.4. Solid-State Characterization

3.4.1. Thermal Analysis by DSC

DSC was used to assess the thermal stability of CSD formulations. It also provides information on how crystalline materials melt and re-crystalline. DSC investigations are therefore helpful in understanding the crystallinity features of CSDs. Figure 5 illustrates the thermal properties of CA and CSDs. CA (micronized) produced a low-intensity endothermic peak at 83.36˚C, showing that the substance is partially crystallized. The crystallinity of the carriers PEG-4000 and Carplex-67 peaked at 65.71˚C and 97.53˚C, respectively. However, there was no notable peak for CA in the thermograms of CSDs, except for broad endothermic peaks for utilized carriers. CSD-4 and CSD-8 thermograms revealed a broad but smaller endothermic peak correlating to CA's melting point.

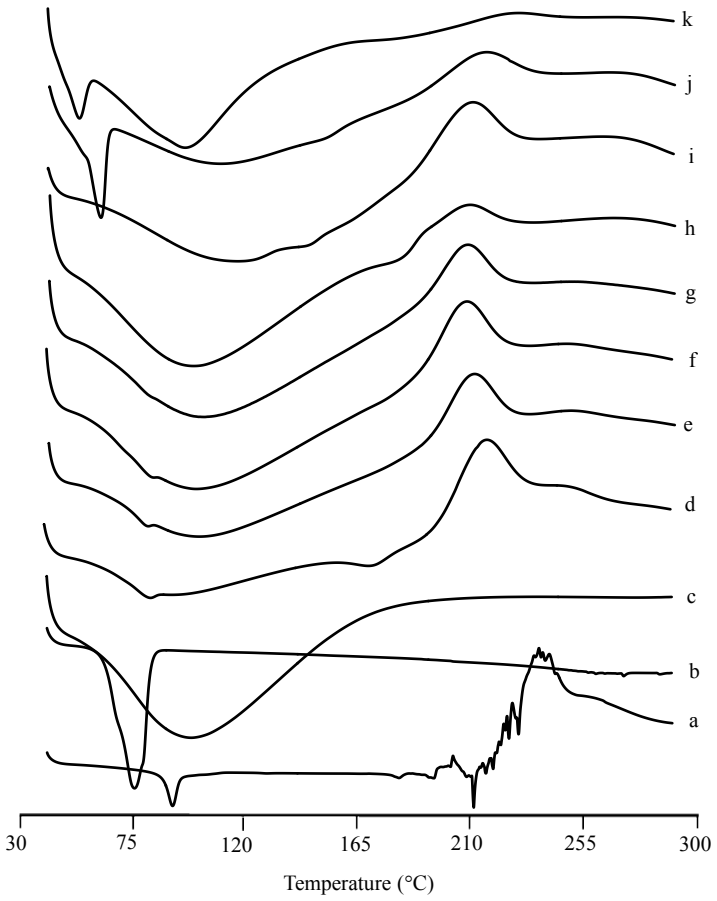

Figure 5. DSC thermos-grams of (a) CA; (b) PEG-4000; (c) Silica; (d) CSD-1; (e) CSD-2; (f) CSD-3; (g) CSD-4; (h) CSD-5; (i) CSD-6; (j) CSD-7; (k) CSD-8.

This finding showed that a portion of CA may undergo amorphous transformation. This solid-state change could happen when SDFs form. However, the thermograms of CSDs revealed that CA had the smallest strong peak, implying that CA could be in an amorphous or molecularly dispersed state. This is due to the high carrier concentration and homogenous medication dispersion on the carrier surface. The possibility of converting CA from a crystalline to an amorphous form during the manufacture of solid dispersions accounts for these results.

3.4.2. Characterization of Crystallinity by PXRD

CA (micronized), silica, PEG, and CSDs powder X-ray diffraction patterns are shown in **Figure 6**. Because of the drug's micronization, the PXRD pattern of CA revealed no major sharp peaks, which matched its DSC thermogram. CA only had a wide peak with an intensity of 21.48 after being micronized. Sharp peaks for PEG were discovered at 2 angles of 19.73˚ and 24.23˚, indicating that PEG-4000 is crystalline.

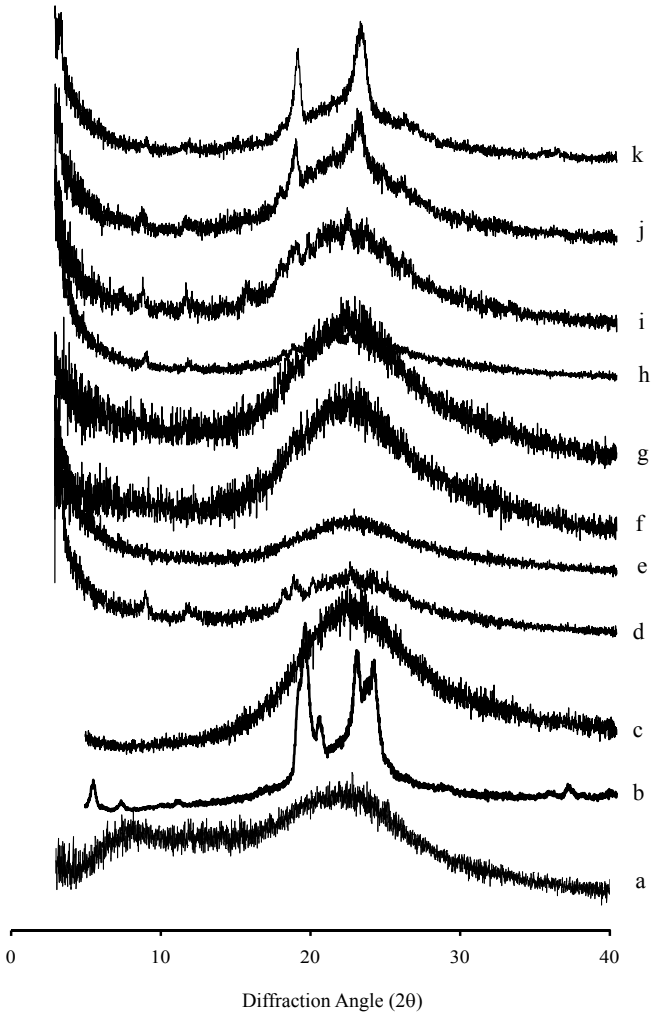

Figure 6. PXRD patterns of (a) CA; (b) Silica; (c) PEG-4000; (d) CSD-1; (e) CSD-2; (f) CSD-3; (g) CSD-4; (h) CSD-5; (i) CSD-6; (j) CSD-7; (k) CSD-8.

However, due to its vast surface area and tiny particle size, silica has no distinct peak and is amorphous in nature. CSD-1, CSD-2, and CSD-5 all have a steep peak. CSD-3, CSD-4, and CSD-6, on the other hand, have a broadened peak at 23.59˚. There was no peak for crystallinity in the instance of CSD-8. The magnitude of the diffraction peaks, on the other hand, demonstrated that the degree of crystallinity of CA in CSD-8 had nearly disappeared. In the CSDs, however, there was no obvious peak for CA. PXRD analysis, like DSC analysis, indicated the change of CA to an amorphous form.

3.4.3. Interaction Study by FTIR

An investigation of probable physicochemical interactions of CA with the carriers was conducted using FTIR spectroscopy. **Figure 7** shows the results of FTIR spectroscopy on CA, silica, PEG-4000, and CSDs.

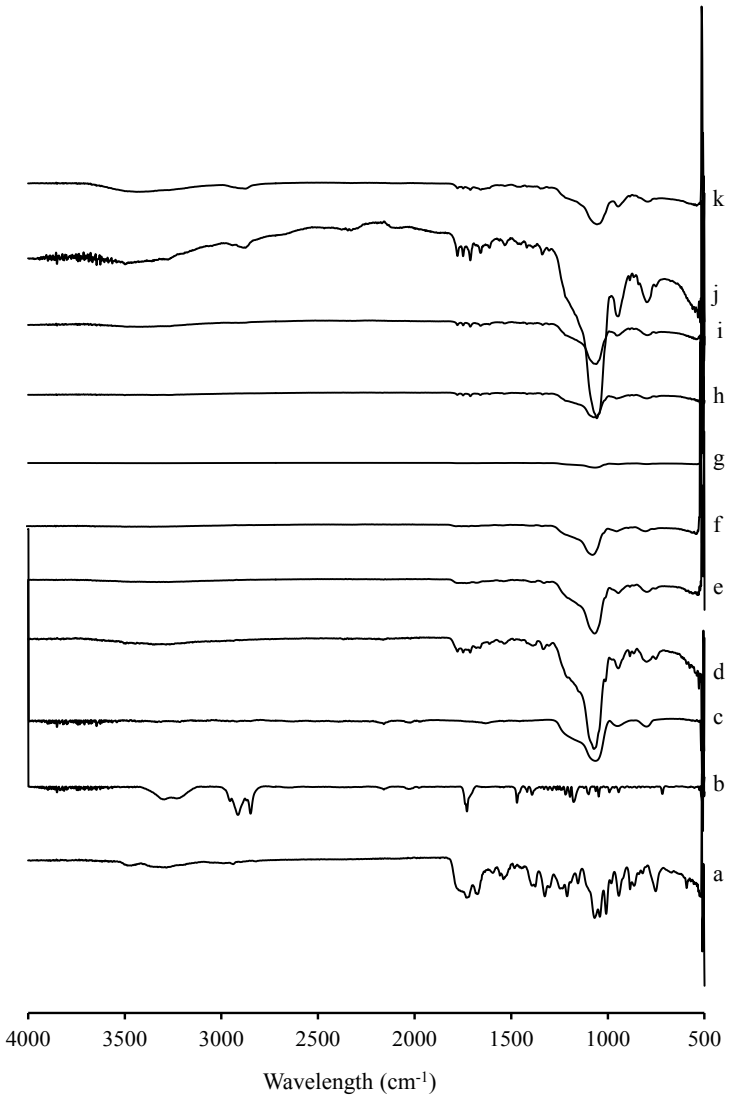

Figure 7. FTIR spectra of (a) CA; (b) PEG-4000; (c) Silica; (d) CSD-1; (e) CSD-2; (f) CSD-3; (g) CSD-4; (h) (i) CSD-6; (j) CSD-7; (k) CSD-8.

CA revealed two absorption bands corresponding to carbonyl groups at 1678 and 1680 cm^{-1}, respectively, assigned to amide (N-H) and carbonyl (C=O) stretching, 1782 cm^{-1} (for lactam), 1760 cm^{-1} (for acetate), 1720 cm^{-1} (for 4-ester group), 1676 cm^{-1} and 1534 cm^{-1} (for 7-amido) [23]. The deformation of the –OH group of Si-OH caused a band at 1055 cm^{-1} and a dramatic decrease in the strength of the Si-OH band at 950 cm^{-1} [24]. For C-H stretching, C-H bending, C-O-H stretching, and O-H stretching, PEG revealed bands at 2876, 1340, 1278, and 1096 cm^{-1}, respectively [25] [26].

In the FTIR spectra of CSDs, however, the intensity of the band for stretching the carbonyl group was lowered, and the band due to stretching the –NH was reduced. This could be due to an interaction between CA's amide group and PEG's C-O-H. Furthermore, the bands caused by lactam, esters, and amides were completely eliminated in all formulations.

Because of the presence of O-H groups in the PEG structure, there was a greater chance of weak hydrogen bonds forming with the polar groups of lactam, ester, and amide groups of CA, resulting in lower bond energy and hence increased wettability of the conjugates In CSD-8, the band for the Si-OH group of Silica was moved from 1093 cm^{-1} to 1076 cm^{-1}, likely due to the chemisorption of the conjugate through the –OH group of PEG. As a result, the FTIR spectra of CSDs revealed many probable in teractions between the additives and CA in the formulation, which would be validated by a subsequent NMR analysis.

3.4.4. Morphological Study by SEM

Figure 8 depicts SEM images of CA, PEG, silica, and CSDs. CA showed as regular spherical particles with uniform and smooth surfaces on the microscope (**Figure 7(a)**). Amorphous powder and irregularly shaped crystals were visible in the SEM pictures of silica and PEG, respectively (**Figure 7(b)**, **Figure 7(c)**) However, no particle of CA was visible in the micrographs of CSDs (**Figures 7(d)-(k)**), indicating that CA molecules may have adsorbed on the carriers' surfaces which may have contributed to the increased dissolution rate of CA in CSD formulations.

3.5. Comparative Dissolution Study

3.5.1. Dissolution Profiles of CSD-8 with Cefuroxime Axetil Tablets in Water

Table 5 and **Figure 9** show the dissolving characteristics of CSD-8 and marketed tablet dosage forms CAMPs (Cefuroxime Axetil Marketed Products). CSD-8 produced more drug release than marketed dosage forms at the initial sampling point, ranging from 7.56 to 13.25-fold with varying meaningful levels. Furthermore, CSD-8 dissolving concentrations were higher than CAMPs at all other sample sites. CAMP-1, CAMP-2, CAMP-3, and CAMP-4 generated 6.75, 7.33, 9.61, and 9.12 μg/ml, respectively, at the end of 600 minutes, whereas CSD-8 produced a comparable peak drug concentration of 12.26 μg/ml ($p < 001$).

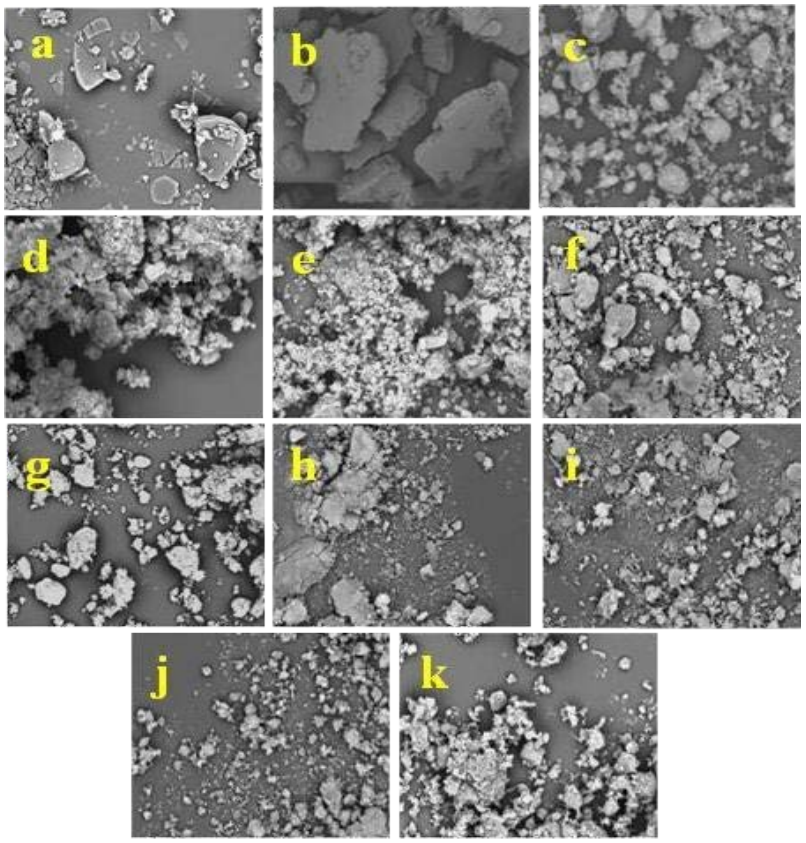

Figure 8. SEM images (×1.0 k); (a) CA; (b) PEG-4000; (c) Silica; (d) CSD-1; (e) CSD-2; (f) CSD-3; (g) CSD-4; (h) CSD-5; (i) CSD-6; (j) CSD-7; (k) CSD-8.

Table 5. Comparative dissolution profiles of CSD-8 with CAMPs in water.

Time (min)	Concentration (μg/ml)				
	CSD-8	CAMP-1	CAMP-2	CAMP-3	CAMP-4
0	0.53 ± 0.02	0.04 ± 0.01*	0.076 ± 0.01**	0.038 ± 0.01*	0.048 ± 0.01*
5	0.63 ± 0.02	0.12 ± 0.02	0.14 ± 0.02	0.17 ± 0.02	0.20 ± 0.02
30	1.15 ± 0.02	0.50 ± 0.03	0.60 ± 0.04	0.60 ± 0.04	0.52 ± 0.04
90	3.28 ± 0.03	1.20 ± 0.02	1.70 ± 0.02	1.84 ± 0.03	1.59 ± 0.10
150	4.93 ± 0.03	2.12 ± 0.05	2.12 ± 0.05	3.30 ± 0.03	2.95 ± 0.03
210	6.34 ± 0.02	2.73 ± 0.03	3.07 ± 0.03	4.55 ± 0.02	4.05 ± 0.05
270	7.85 ± 0.02	3.38 ± 0.03	4.03 ± 0.03	5.69 ± 0.01	5.06 ± 0.03
330	8.97 ± 0.02	3.97 ± 0.05	4.80 ± 0.04	6.51 ± 0.015	6.01 ± 0.03
420	10.89 ± 0.01	5.06 ± 0.03	5.79 ± 0.01	7.82 ± 0.03	7.24 ± 0.01
510	11.74 ± 0.02	6.06 ± 0.02	6.63 ± 0.02	8.74 ± 0.03	8.36 ± 0.09
600	12.26 ± 0.02	6.75 ± 0.02*	7.33 ± .020*	9.61 ± .05**	9.12 ± .03**

Results are presented as mean ± S.E.M. *p < 0.05, **p < 0.01, ***p < 0.001 vs. CSD-8.

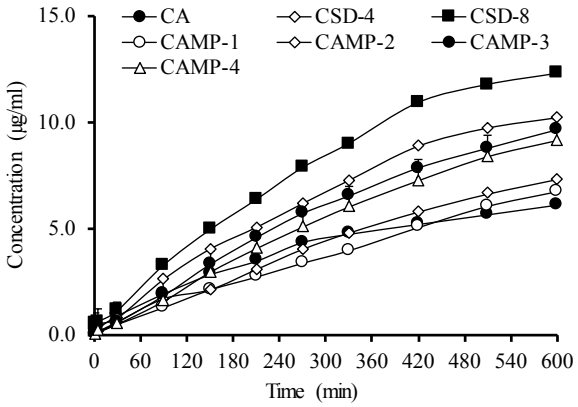

Figure 9. Dissolution profile of CSD-4, CSD-8, CAMP-1, CAMP-2, CAMP-3, and CAMP-4 in water. Each value represents mean ± S.E.M (n = 3).

3.5.2. Dissolution Profiles of CSD-8 with Cefuroxime Axetil Tablets in GSF

Dissolution profiles of CSD-8 and marketed tablet dosage forms are depicted in **Table 6** and **Figure 10**. In this profile, drug release from CSD-8 was comparatively lower at all sampling points than the CAMPs in GSF. However, the drug concentration of CSD-8 was comparable with that of CAMP-4 at 600 minutes.

3.5.3. Dissolution Profiles of CSD-8 with Cefuroxime Axetil Tablets in ISF

Table 7 and **Figure 11** show the comparison of CSD-8 and CAMPs dissolution in phosphate buffer pH 6.8 media. CSD-8 released much more drugs ($p < 0.001$) than CAMPs at the initial sampling point, ranging from 1.91 to 5.50-fold. Furthermore, at all sample points, CSD-8 showed significantly higher drug concentrations than marketed dosage forms.

4. Discussion

Cefuroxime Axetil (CA) is a BCS class II drug having very poor aqueous solubility that plays a limiting role on its bioavailability [26]. To overcome this limitation solid dispersion (SD) formulations were developed to enhance the aqueous solubility and hence bioavailability of this hydrophobic drug. For this, various formulations of CSDs were prepared using PEG-4000 and Carplex-67 as carrier. The resultant CSD formulations were characterized and evaluated through *in-vitro* dissolution and solid state characterization by DSC, PXRD, FTIR and SEM. From the *in-vitro* dissolution study, it can be seen that the drug release concentration obtained from the silica-based formulation CSD-4 was 10.21 µg/ml, which was 1.75 times higher than that of pure CA. At 600 minutes, adding PEG 4000 to formulation CSD-8 resulted in a medication concentration of 12.26 µg/ml, which was 2.11 times greater than pure CA (**Table 3** & **Table 4** and **Figure 3** & **Figure 4**). Increased hydrophilicity was accomplished with the use of PEG, a hydrophilic polymer, which facilitated CA dissolution. This could be due to chemisorptions on PEG and silica, as well as improved drug wettability, as

shown by physicochemical analysis. The conversion of the drug from crystalline to amorphous form was demonstrated by DSC thermograms (**Figure 5**) of the CSDs, as well as PXRD (**Figure 6**) data. The other mechanism, physical bonding between carriers and pharmaceuticals, was demonstrated by FTIR spectrum (**Figure 7**), implying that this interaction could improve the drug's wettability qualities and raise drug dissolution rates [27] [28].

Table 6. Comparative dissolution profiles of CSD-8 with CAMPs in GSF.

Time (min)	Concentration (µg/ml)				
	CSD-8	CAMP-1	CAMP-2	CAMP-3	CAMP-4
0	0.14 ± 0.01	0.88 ± 0.04**	0.61 ± 0.01*	0.93 ± 0.05***	0.90 ± 0.03***
5	0.25 ± 0.03	1.01 ± 0.03	1.25 ± 0.01	1.23 ± 0.01	1.25 ± 0.01
30	1.05 ± 0.01	2.67 ± 0.01	1.94 ± 0.03	1.81 ± 0.01	2.35 ± 0.02
90	2.93 ± 0.03	4.76 ± 0.03	4.18 ± 0.04	2.93 ± 0.04	3.89 ± 0.03
150	4.30 ± 0.02	6.27 ± 0.05	6.30 ± 0.02	6.33 ± 0.01	4.33 ± 0.01
210	5.61 ± 0.04	7.26 ± 0.01	7.99 ± 0.01	7.70 ± 0.02	4.76 ± 0.02
270	6.75 ± 0.03	8.43 ± 0.01	9.16 ± 0.03	8.57 ± 0.03	5.74 ± 0.05
330	7.75 ± 0.01	9.09 ± 0.02	10.55 ± 0.01	9.59 ± 0.01	6.33 ± 0.06
420	9.06 ± 0.02	9.76 ± 0.03	12.20 ± 0.03	11.59 ± 0.05	7.85 ± 0.02
510	9.83 ± 0.03	10.92 ± 0.03	13.47 ± 0.02	12.99 ± 0.03	9.05 ± 0.01
600	10.29 ± 0.03	11.25 ± 0.02**	13.75 ± 0.03***	13.29 ± 0.02***	9.12 ± 0.02*

Results are presented as mean ± S.E.M. *p < 0.05, **p < 0.01, ***p < 0.001 vs. CSD-8.

Table 7. Comparative dissolution profiles of CSD-8 with CAMPs in ISF.

Time (min)	Concentration (µg/ml)				
	CSD-8	CAMP-1	CAMP-2	CAMP-3	CAMP-4
0	0.44 ± 0.01	0.23 ± 0.03**	0.11 ± 0.01*	0.16 ± 0.03*	0.08 ± 0.01*
5	0.68 ± 0.01	0.41 ± 0.03	0.14 ± 0.01	0.32 ± 0.01	0.14 ± 0.03
30	1.46 ± 0.05	0.83 ± 0.01	0.74 ± 0.06	1.28 ± 0.01	0.98 ± 0.01
90	2.88 ± 0.02	2.09 ± 0.05	1.34 ± 0.03	2.48 ± 0.03	2.53 ± 0.01
150	4.42 ± 0.03	2.50 ± 0.04	2.06 ± 0.01	4.18 ± 0.03	3.82 ± 0.05
210	6.21 ± 0.03	3.54 ± 0.03	2.64 ± 0.02	5.31 ± 0.02	4.9 ± 0.04
270	7.35 ± 0.01	3.88 ± 0.01	3.04 ± 0.04	6.00 ± 0.01	5.73 ± 0.02
330	8.27 ± 0.01	4.45 ± 0.11	3.82 ± 0.02	6.96 ± 0.03	6.24 ± 0.01
420	9.35 ± 0.01	5.28 ± 0.01	4.36 ± 0.03	7.70 ± 0.04	7.02 ± 0.01
510	10.08 ± 0.04	5.89 ± 0.01	4.88 ± 0.01	8.10 ± 0.02	7.44 ± 0.05
600	10.18 ± 0.01	6.05 ± 0.05*	5.33 ± 0.05*	8.33 ± 0.01**	8.09 ± 0.01**

Results are presented as mean ± S.E.M. *p < 0.05, **p < 0.01, ***p < 0.001 vs. CSD-8.

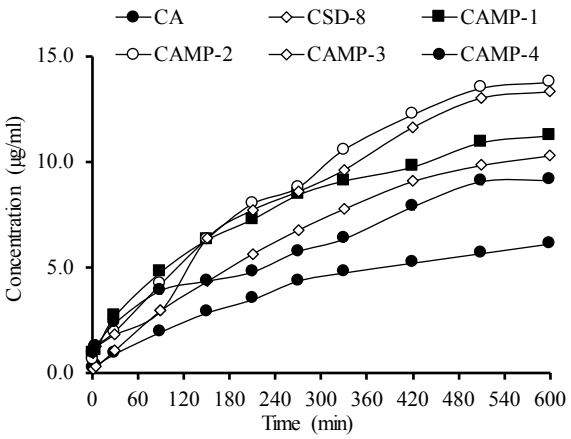

Figure 10. Dissolution profile of CSD-4, CSD-8, CAMP-1, CAMP-2, CAMP-3 CAMP-4 in GSF. Each value represents mean ± S.E.M (n = 3).

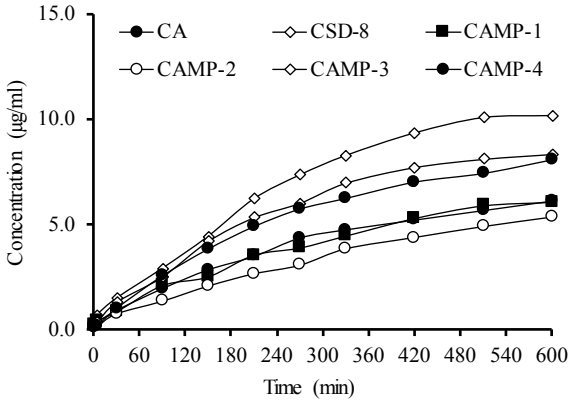

Figure 11. Dissolution profile of CSD-4, CSD-8, CAMP-1, CAMP-2, CAMP-3, and CAMP-4 in ISF. Each value represents mean ± S.E.M (n = 3).

DSC, PXRD, and SEM pictures combined showed that the hydrophilic carriers reduced the crystalline behaviour of CA in the CSDs to varying degrees. Physical change (from micronized to amorphous) and adsorptions of CA on the surface of the carrier molecules by weak H-bonding between the –O-H groups of PEG, silica, and the displayed functional groups of the drug could be the cause of this conversion. CSDs improved drug release profile could be the result of interaction-mediated adsorptions to varying degrees. Furthermore, CSD-8 (**Figure 8(k)**) revealed a network-like structure that promoted water absorption, resulting in rapid and improved CA dissolution. Based on its dissolution behaviour, DSC, PXRD, FTIR, and SEM data, CSD-8 can be recognized as the best solid dispersion formulation among the CSDs.

In a comparative dissolution analysis with commercialized cefuroxime axetil tablets using water, GSF, and ISF, CSD-8 produced significantly greater drug release ($p < 0.01$) in aqueous and ISF media, respectively (**Table 5** & **Table 7** and **Figure 9** & **Figure 11**). This is most likely owing to the presence of PEG 4000 in

the formulation, which has a controlled release feature. Because cefuroxime is readily absorbed via the intestinal mucosa after hydrolysis by esterase from its 1-acetoxyethyl ester form [29], the recently discovered CSD-8 looks promising for ensuring its oral bioavailability, even though the drug release concentration in GSF is lower (**Table 6** and **Figure 10**). This may make it easier to prevent CA metabolism in the first-pass metabolism, resulting in optimal systemic bioavailability.

In a previous study, researchers used a combination of fusion and surface adsorption to improve the dissolution of a poorly water-soluble drug CA, where poloxamer 188 plays a key role in drug solubility and dissolution and surface adsorbent, Neusilin US2 may be used to give solid dispersions good flow and compressibility. Neusilin US2 also increases effective surface area, which improves the dissolving rate. The combination of fusion and surface adsorption has been successfully employed to improve the solubility rate of the BCS class II medication CA [30].

Another study indicated that using a solid dispersion technique for creating solid dispersion formulations of the poorly water-soluble drug CA with polyvinyl pyrrolidone (PVP K 30) and polyethelene glycol 4000 led to enhanced solubility, which in turn boosted dissolution rate [23]. The dissolving rate of CA was enhanced by employing the solvent evaporation method to prepare solid dispersion with urea, according to Irchhaiya R *et al.* (2010) [31]. Dinda SC *et al.* (2012) also found that employing porous carrier sylysia 350 to prepare solid dispersions enhanced CA solubility, dissolution rate, flowability, and compressibility significantly [32]. Salam MT *et al.* (2020) suggested a solid dispersion formulation with improved solubility and antibacterial action employing microcrystalline cellulose (Avicel PH 102) as the carrier [33].

The current study's findings that formulations produced using the dispersion method and carriers showed a significant improvement in dissolution rate is supported by all of these results. This might increase absorption and, thus, the bioavailability of CA, which can be verified by additional *in-vivo* bioavailability research.

5. Conclusions

In conclusion, CSD-8 was determined to be a superior formulation in terms of dissolution rate to the existing tablet dosage forms. As a result, CSD-8 may be a viable alternative to traditional CA dosage formulations.

However, before CSD-8 can be considered as a novel formulation, more *in-vivo* research is needed to confirm its pharmacokinetics and antibacterial activity, as well as its safety margin.

Acknowledgements

We gratefully acknowledge Professor Hiromu Kondo, Department of Pharmaceutical Engineering and Drug Delivery Science, University of Shizuoka, Japan,

and the National Science and Technology (NST) Division of the Ministry of Science and Technology of the People's Republic of Bangladesh for providing an NST scholarship to support this research.

Conflicts of Interest

The authors declare no conflicts of interest regarding the publication of this paper.

References

[1] Dhumal, R.S., Biradar, S.V., Aher, S. and Paradkar, A.R. (2009) Cefuroxime Axetil Solid Dispersion with Polyglycolized Glycerides for Improved Stability and Bioavailability. *Journal of Pharmacy and Pharmacology*, **61**, 743-751. https://doi.org/10.1211/jpp.61.06.0006

[2] National Center for Biotechnology Information (2023) Cefuroxime Axetil. https://pubchem.ncbi.nlm.nih.gov/compound/Cefuroxime-axetil

[3] Pichichero, M.E. (2006) Cephalosporins Can Be Prescribed Safely for Penicillin-Allergic Patients. *The Journal of Family Practice*, **55**, 106-112.

[4] Dhumal, R.S., Biradar, S.V., Yamamura, S., Paradkar, A.R. and York, P. (2008) Preparation of Amorphous Cefuroxime Axetil Nanoparticles by Sonoprecipitation for Enhancement of Bioavailability. *European Journal of Pharmaceutics and Biopharmaceutics*, **70**, 109-115. https://doi.org/10.1016/j.ejpb.2008.04.001

[5] Zhang, X., Xing, H., Zhao, Y. and Ma, Z. (2018) Pharmaceuticals Dispersion Techniques for Dissolution and Bioavailability Enhancement of Poorly Water-Soluble Drugs. *Pharmaceutics*, **10**, Article 74. https://doi.org/10.3390/pharmaceutics10030074

[6] Singh, A., Worku, Z.A. and Van den Mooter, G. (2011) Oral Formulation Strategies to Improve the Solubility of Poorly Water-Soluble Drugs. *Expert Opinion on Drug Delivery*, **8**, 1361-1378. https://doi.org/10.1517/17425247.2011.606808

[7] Chiou, W.L. and Riegelman, S. (1971) Pharmaceutical Applications of Solid Dispersion Systems. *Journal of Pharmaceutical Sciences*, **60**, 1281-1302. https://doi.org/10.1002/jps.2600600902

[8] Huang, Y. and Dai, W.G. (2014) Fundamental Aspects of Solid Dispersion Technology for Poorly Soluble Drugs. *Acta Pharmaceutica Sinica B*, **4**, 18-25. https://doi.org/10.1016/j.apsb.2013.11.001

[9] Sridhar, I., Doshi, A., Joshi, B., Wankhede, V. and Doshi, J. (2013) Solid Dispersions: An Approach to Enhance the Solubility of the Poorly Water-Soluble Drug. *International Journal of Innovation Science and Research*, **2**, 685-694.

[10] Thenmozhi, K. and Yoo, Y.J. (2017) Enhanced Solubility of Piperine Using Hydrophilic Carrier-Based Potent Solid Dispersion Systems. *Drug Development and Industrial Pharmacy*, **43**, 1501-1509. https://doi.org/10.1080/03639045.2017.1321658

[11] Yamashita, K., Nakate, T., Okimoto, K., Ohike, A., Tokunaga, Y., Ibuki, R., Higaki, K. and Kimura, T. (2003) Establishment of New Preparation Method for Solid Dispersion Formulation of Tacrolimus. *International Journal of Pharmaceutics*, **267**, 79-91. https://doi.org/10.1016/j.ijpharm.2003.07.010

[12] Leuner, C. and Dressman, J. (2000) Improving Drug Solubility for Oral Delivery Using Solid Dispersions. *European Journal of Pharmaceutics and Biopharmaceutics*, **50**, 47-60. https://doi.org/10.1016/S0939-6411(00)00076-X

[13] Lavra, Z.M.M., Pereira de Santana, D. and Inês Ré, M. (2017) Solubility and Dissolution Performances of Spray-Dried Solid Dispersion of Efavirenz in Soluplus. *Drug Development and Industrial Pharmacy*, **43**, 42-54. https://doi.org/10.1080/03639045.2016.1205598

[14] Qi, S., Gryczke, A., Belton, P. and Craig, D.Q. (2008) Characterisation of Solid Dispersions of Paracetamol and EUDRAGIT® E Prepared by Hot-Melt Extrusion Using Thermal, Microthermal, and Spectroscopic Analysis. *International Journal of Pharmaceutics*, **354**, 158-167. https://doi.org/10.1016/j.ijpharm.2007.11.048

[15] Mouffok, M., Mesli, A., Abdelmalek, I. and Gontier, E. (2016) Effect of the Formulation Parameters on the Encapsulation Efficiency and Release Behavior of p-Aminobenzoic Acid-Loaded Ethylcellulose Microspheres. *Journal of the Serbian Chemical Society*, **81**, 1183-1198. https://doi.org/10.2298/JSC160308068M

[16] Mauger, J., Ballard, J., Brockson, R., De, S., Gray, V. and Robinson, D. (2003) Intrinsic Dissolution Performance Testing of the USP Dissolution Apparatus 2 (Rotating Paddle) Using Modified Salicylic Acid Calibrator Tablets: Proof of Principle. *Dissolution Technologies*, **10**, 6-15. https://doi.org/10.14227/DT100303P6

[17] Matkar, R.D., Dagadiye, R.B., Kajale, A.D. and Mahajan, V.K. (2012) USP/IP/NON-USP Dissolution Apparatus. *International Journal of Pharmacy and Life Sciences*, **2**, 40-67.

[18] Barman, R.K., Iwao, Y., Funakoshi, Y., Ranneh, A.H., Noguchi, S., Wahed, M.I. and Itai, S. (2014) Development of Highly Stable Nifedipine Solid-Lipid Nanoparticles. *Chemical and Pharmaceutical Bulletin*, **62**, 399-406. https://doi.org/10.1248/cpb.c13-00684

[19] Jaymin, C., Shah, J.R. and Chen, D.C. (1995) Preformulation Study of Etoposide: II. Increased Solubility and Dissolution Rate by Solid-Solid Dispersions. *International Journal of Pharmaceutics*, **113**, 103-111. https://doi.org/10.1016/0378-5173(94)00195-B

[20] Palmieri, G.F., Antonini, I. and Martelli, S. (1996) Characterization and Dissolution Studies of PEG 4000. *STP Pharma Sciences*, **6**, 188-194.

[21] Calis, S., Atar, K.O., Arslan, F.B., Eroğlu, H. and Çapan, Y. (2019) Nanopharmaceuticals as Drug-Delivery Systems: For, Against, and Current Applications. In: Mohapatra, S.S., Ranjan, S., Dasgupta, N., Mishra, R.K. and Thomas, S., Eds., *Nanocarriers for Drug Delivery*, Elsevier, Ankara, 133-144. https://doi.org/10.1016/B978-0-12-814033-8.00004-7

[22] Honary, S., Ebrahimi, P. and Hadianamrei, R. (2014) Optimization of Particle Size and Encapsulation Efficiency of Vancomycin Nanoparticles by Response Surface Technology. *Pharmaceutical Development and Technology*, **19**, 987-998. https://doi.org/10.3109/10837450.2013.846375

[23] Gorajana, A., Rajendran, A., Yew, L.M. and Dua, K. (2015) Preparation and Characterization of Cefuroxime Axetil Solid Dispersions Using Hydrophilic Carriers. *International Journal of Pharmaceutical Investigation*, **5**, 171-178. https://doi.org/10.4103/2230-973X.160857

[24] Chukin, G.D. and Malevich, V.I. (1977) Infrared Spectra of Silica. *Journal of Applied Spectroscopy*, **26**, 223-229. https://doi.org/10.1007/BF00615613

[25] Shameli, K., Bin Ahmad, M., Jazayeri, S.D., Sedaghat, S., Shabanzadeh, P., Jahangirian, H., Mahdavi, M. and Abdollahi, Y. (2012) Synthesis and Characterization of Polyethylene Glycol-Mediated Silver Nanoparticles by the Green Method. *International Journal of Molecular Science*, **13**, 6639-6650. https://doi.org/10.3390/ijms13066639

[26] Panigrahi, K.C., Sruti, J., Patra, C.N., Swain, S., Patro, A.P., Beg, S., Dinda, S.C. and

Rao, M.E. (2013) Improvement in the Dissolution Rate and Tableting Properties of Cefuroxime Axetil by Melt-Granulated Dispersion and Surface Adsorption. *Acta Pharmaceutica Sinica B*, **3**, 113-122. https://doi.org/10.1016/j.apsb.2013.01.001

[27] Patel, J.R., Carlton, R.A., Yuniatine, F., Needham, T.E., Wu, L. and Vogt, F.G. (2012) Preparation and Structural Characterization of Amorphous Spray-Dried Dispersions of Tenoxicam with Enhanced Dissolution. *Journal of Pharmaceutical Sciences*, **101**, 641-663. https://doi.org/10.1002/jps.22800

[28] Pahovnik, D., Reven, S., Grdadolnik, J., Mavri, J. and Zagar, E. (2011) Determination of the Interaction between Glimepiride and Hyperbranched Polymers in Solid Dispersions. *Journal of Pharmaceutical Sciences*, **100**, 4700-4709. https://doi.org/10.1002/jps.22662

[29] Harding, S.M., Williams, P.E. and Ayrton, J. (1984) Pharmacology of Cefuroxime as the 1-Acetoxyethyl Ester in Volunteers. *Antimicrobial Agents and Chemotherapy*, **25**, 78-82. https://doi.org/10.1128/AAC.25.1.78

[30] Sruti, J., Patra, C.N., Swain, S.K., Beg, S., Palatasingh, H.R., Dinda, S.C., *et al.* (2013) Improvement in Dissolution Rate of Cefuroxime Axetil by Using Poloxamer 188 and Neusilin US2. *Indian Journal of Pharmaceutical Sciences*, **75**, 67-75. https://doi.org/10.4103/0250-474X.113551

[31] Arora, S.C., Sharma, P.K., Irchhaiya, R., Khatkar, A., Singh, N. and Gagoria, J. (2010) Development, Characterization and Solubility Study of Solid Dispersions of Cefuroxime Axetil by the Solvent Evaporation Method. *Journal of Advanced Pharmaceutical Technology & Research*, **1**, 326-329.

[32] Sruti, J., Patra, C.N., Swain, S., Dinda, S.C., Eswar, M. and Rao, B. (2012) Cefuroxime Axetil Dissolution Improvement by Preparation of Solid Dispersions with the Porous Carrier. *Journal of Advanced Pharmacy Research*, **3**, 42-48.

[33] Salam, M.T., Kumar, A., Hata, A., Kondo, H., Salam, M.A., Wahed, M.I.I., Khan, M.R.I. and Barman, R.K. (2020) Accelerated Dissolution and Antibacterial Activity of Cefuroxime Axetil Using Microcrystalline Cellulose as a Carrier. *Pharmacology & Pharmacy*, **11**, 159-173. https://doi.org/10.4236/pp.2020.118015